

## Bioelectrical Analysis of Swab Samples During and After Viral Nasopharyngitis Infection Using a Variable Impedance Module

Christian Lexequías \*<sup>1</sup>, Bryan Urcia<sup>1</sup>, Nicole Morante<sup>1</sup>, Sara Díaz<sup>1</sup>, Oscar Baltuano<sup>1,2</sup> and Galo Patiño<sup>1</sup>

<sup>1</sup> Universidad Nacional Mayor de San Marcos, Grupo de investigación INFISA, Lima, Perú

<sup>2</sup> Dirección de Investigación y Desarrollo, Instituto Peruano de Energía Nuclear, Lima, Perú.

Recibido 12 Jun 2024 – Aceptado 24 Feb 2025 – Publicado 01 Abr 2025

### Abstract

This research shows the bioelectrical characterization and impedance reading of nasopharyngeal samples taken during the infection stage of a patient with viral rhinopharyngitis compared to the healthy stage of the same patient. Eleven nasopharyngeal samples were taken during the initial phase of infection and 10 nasopharyngeal samples 14 days after not presenting any symptoms. The analysis was carried out in a frequency range of 10 kHz - 1 MHz using the MIVA (Module of Variable Impedance for Analysis) bioelectrical impedance equipment. The results obtained indicated a significant difference in the impedance of the samples during the different stages, which allowed establishing a range in the axes ( $Z'$  and  $Z''$ ) of the Nyquist diagram when a nasopharyngeal sample comes from a case of viral rhinopharyngitis and when the sample comes from a healthy patient. In addition, it will be modified to schematize a circuit equivalent to the bioelectric behavior of the sample with the respective value of its components, which will greatly help for future research that wishes to work in the same field of study.

**Keywords:** Characterization, bioelectric, viral rhinopharyngitis, impedance, diagnosis.

### Análisis bioeléctrico de muestras de hisopado durante y después de la infección con rinofaringitis viral mediante un Módulo de Impedancia Variable

#### Resumen

Esta investigación muestra la caracterización bioeléctrica y lectura de impedancia de muestras nasofaríngeas tomadas durante la etapa de infección de un paciente con rinofaringitis viral comparada con la etapa saludable del mismo paciente. Se tomaron 11 muestras nasofaríngeas durante la fase inicial de infección y 10 muestras nasofaríngeas 14 días después de no presentar ningún síntoma. El análisis se llevó a cabo en un rango de frecuencias de 10 kHz - 1 MHz haciendo uso del equipo de impedancia bioeléctrica MIVA (Módulo de Impedancia Variable para Análisis). Los resultados obtenidos indicaron una diferencia significativa en la impedancia de las muestras durante las distintas etapas, lo cual permitió establecer un rango en los ejes ( $Z'$  y  $Z''$ ) del diagrama de Nyquist cuando una muestra nasofaríngea proviene de un caso de rinofaringitis viral y cuando la muestra proviene de un paciente sano. Además, se logró esquematizar un circuito equivalente al comportamiento bioeléctrico de la muestra con el respectivo valor de sus componentes, lo cual ayudará en gran medida para futuras investigaciones que se deseen trabajar en el mismo campo de estudio.

**Palabras clave:** Caracterización, bioeléctrica, rinofaringitis viral, impedancia, diagnóstico.

\*lexekyas@gmail.com

© Los autores. Este es un artículo de acceso abierto, distribuido bajo los términos de la licencia Creative Commons Atribución 4.0 Internacional (CC BY 4.0) que permite el uso, distribución y reproducción en cualquier medio, siempre que la obra original sea debidamente citada de su fuente original.



## Introduction

At present, there are diseases that require invasive methods to be diagnosed. Due to this, since 2019, the Research Group (GI) INFISA has been carrying out studies aimed at finding non-invasive methods to detect diseases during biotechnological and medical applications. As a result of these studies, it was possible to achieve the development of equipment capable of reading biological material using the Electrical Impedance Spectroscopy (EIS) method.

The EIS is a technique from the field of Physics that uses the concept of impedance to characterize the electrical behavior of a material [1, 2]. In the Technological Biophysics and Medical Applications research area, this technique takes the name of Bioelectrical Impedance Analysis (BIA) [3,4], which has allowed through multiple applications to analyze the bioelectric behavior in samples of stem cells from adipose tissue [5], blood platelet aggregometry [6], detection of bacterial cells [7], tomography in acute lung injury [8] and human immunodeficiency virus type 1 assay [9]. The mentioned studies obtained optimal data fulfilling their research objectives; however, all investigations have the problem of high cost to perform the analysis that results in the complication of its application as a possible diagnostic method.

The MIVA or Variable Impedance Module for Analysis is a bioelectrical impedance spectroscopy kit designed, developed, and assembled at the INFISA GI. This equipment is intended to be a cheaper option for BIA studies. Its operation is based on applying an alternating current with a positive potential difference in a range of less than 5 V to a biological material with a volume of 0.6  $\mu$ L. The signal received by the equipment measures the ease that the sample presents to the passage of the current, knowing this phenomenon as the Admittance (Y) [10]. The impedance (Z) being the opposition to the passage of alternating current that the material presents, is found as the inverse of the Admittance [11] shown in equation (1).

$$Z = \frac{1}{Y} \quad (1)$$

This equation is the simplified formulation of the inverse of the admittance to find the impedance which is programmed in the MIVA kit.

Once the data has been obtained by MIVA, the spectra that relate the impedance components (Resistance and Reactance) can be observed, reflected in an Argand diagram known as Nyquist [12]. In addition, we can also observe the Bode diagram that corresponds to the sum of two graphs that show the impedance module ( $|Z|$ ) and the phase angle ( $\theta^\circ$ ) with respect to the frequency change [13]. Using this method, the techno-

logical kit has managed to perform readings in blood tissue with optimal results, finding differences between the impedance spectra in patients with different amounts of hemoglobin [14]. He was also able to read the enzyme glucose oxidase (GOx) where differences were found in relation to its concentration in an aqueous solution [15].

This research carries out a study on nasopharyngeal samples with the objective of finding differences between the bioelectric responses of a patient during the stage of viral rhinopharyngitis and the stage of the same patient during his normal health considered as "healthy or healthy". Viral rhinopharyngitis is taken into consideration for its BIA study because it is a disease that is easy to control by health [16] and belongs to the most frequent respiratory infections for public health [17, 18].

Finally, the data presented is expected to be of great use to the growing branch of Biophysics that involves the BIA study as a vision to develop a reliable diagnostic method and possible treatment of current and future diseases.

This work is part of the vision of the INFISA Research Group to develop a less invasive method for the diagnosis of diseases that affect the respiratory and circulatory systems.

## Materials and Methods

### MIVA preparation:

Power and data feed connections were assembled on a computer running Windows operating system. The equipment used 5 V power for its operation, which was from the same source as the computer. The supplied voltage has no significance to the current used during the BIA study other than just turning on the internal circuitry. Making use of the free software program WaveForms [19] as controller of the equipment, we proceeded to make the revision settings for its correct operation. These adjustments consist in the automatic recognition of the equipment by the software and the analysis of the amount of voltage that it has of power. Eventually, the equipment was calibrated between its maximum and minimum frequency range applied in a parallel R(resistance)-C(Capacitance) pattern circuit, expecting as a result a semicircle plotted on the Nyquist diagram (Figure 1). This graph with a semicircular trend indicates the proper functioning of the equipment to take readings because it corresponds to the model known as Cole-Cole and is considered for basic impedance studies in biological tissues with an internal R-C circuit [20]. As a result, the Variable Impedance Module for Analysis (MIVA) was obtained, which was covered by a 3D printed structure (Figure 2).

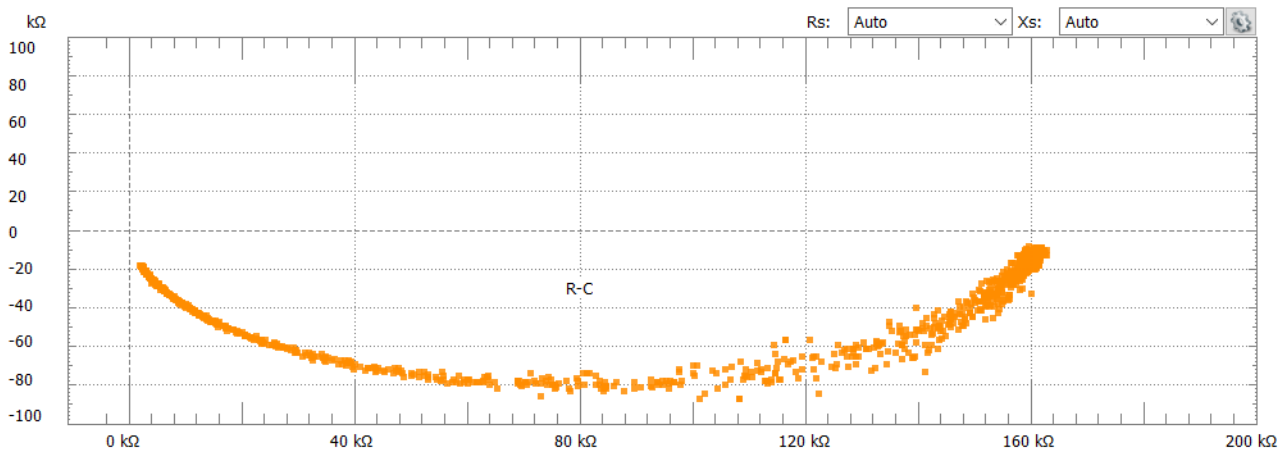


**Figure 1:** Nyquist plot corresponding to the R-C parallel circuit with Color Bk Light and plot Width of 4. This image was taken directly from how it is seen in the WaveForms software during the calibration stage.



**Figure 2:** Prototype of the variable impedance module for analysis (MIVA) used in the research.

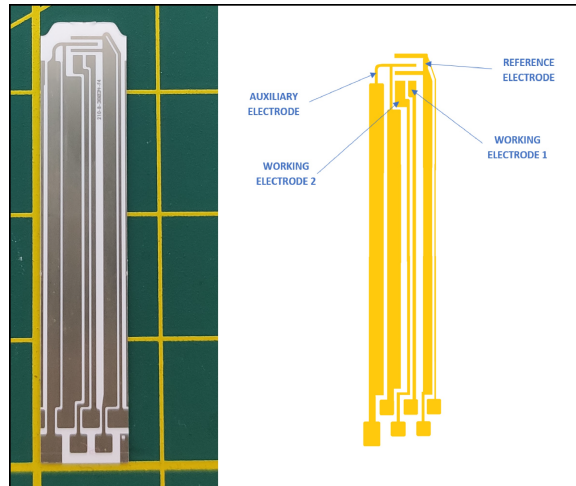


**Figure 3:** Measurement arrangement of the extensions of the microelectrode obtained from the Accu-Check® Performa test strips (Made in GIMP).

**Microelectrodes for BIA measurement:**

In order to perform readings using the MIVA equipment, microelectrodes with 6 hook terminals and a dimension of 7 mm x 35 mm were used. For this research, Accu-Check® Performa test strips were used because, through their internal modification, a stable microelectrode could be obtained to read bioelectrical analysis; however, no type of pathological receptor was used for this project [21] (Figure 3). In addition, the cost of test strips and their ease of disposal allow us to maintain adequate sanitary control according to the parameters established by the National Institute of Health of Peru.

**Sample preparation:**

For sample collection, the nasopharyngeal swab methodology was used, which has previously been used for virus detection by direct immunofluorescence [22]. Eleven nasopharyngeal swab samples were taken from a patient with a clinical diagnosis of early-stage viral rhinopharyngitis. The samples were each deposited in a different sterile container. For the bioelectric reading using the MIVA equipment, a syringe was used that transported an approximate amount of 0.6 uL of sample from the sterile vial to the microelectrode (Figure 4). After this first extraction, the appropriate follow-up control and treatment of the patient was carried out, taking into account the etiological agent and its incubation period. In this case, the etiological agent was Rhinovirus with an

incubation period of between 1 and 4 days [23,24], being the cause of viral rhinopharyngitis or common cold.



**Figure 4:** Image of the moment in which the biological sample of viral rhinopharyngitis extracted is placed on the electrode.

Once the illness was overcome, he waited 14 days, registering that he did not present any symptoms of viral rhinopharyngitis or other illness. After this stage, 10 nasopharyngeal samples were collected for their respective bioelectrical reading.

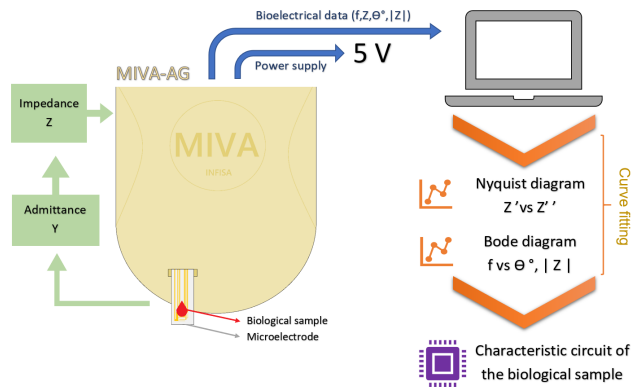


**Figure 5:** Simplified scheme of the bioelectrical characterization using the MIVA-AG equipment.

### Configuration and data processing:

To perform the bioelectrical analysis, the MIVA kit was configured to apply an alternating current with a positive potential difference of 100 mV in a frequency range of 10 kHz to 1 MHz. For the analysis, these values were established considering the impedance parameters for the virus study [25] and previous experimentation with biological material developed in the INFISA laboratory. Once the electrical data ( $Z$ ,  $\theta^\circ$ ,  $|Z|$ ) was obtained, we proceeded to data processing and curve fitting using the Zview program [26]. In this curve fitting step, an electrical circuit value was assigned in accordance with the Nyquist and Bode plot behavior of each sample. In this way, the internal components of the sample and its

biological characterization as an electrical circuit were found (Figure 5).

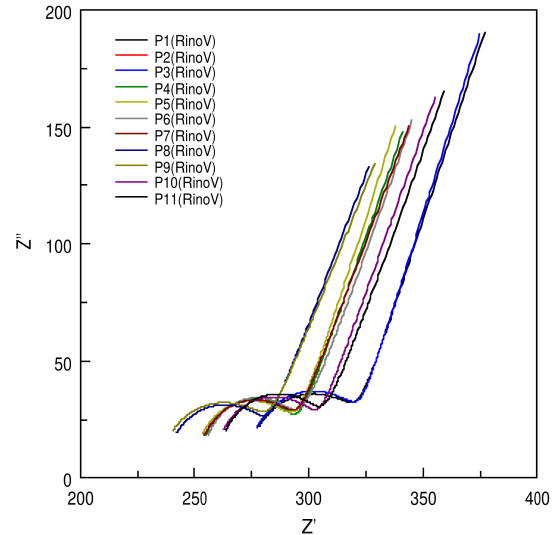


**Figure 6:** Nyquist diagram corresponding to the 11 samples of viral rhinopharyngitis (Prepared in Zview).

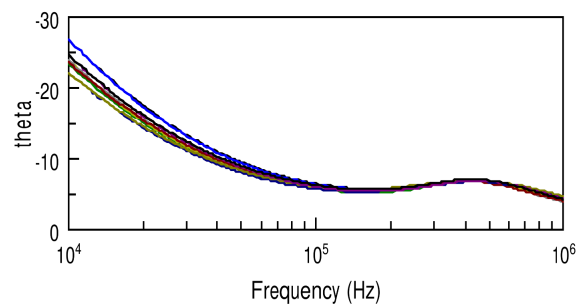
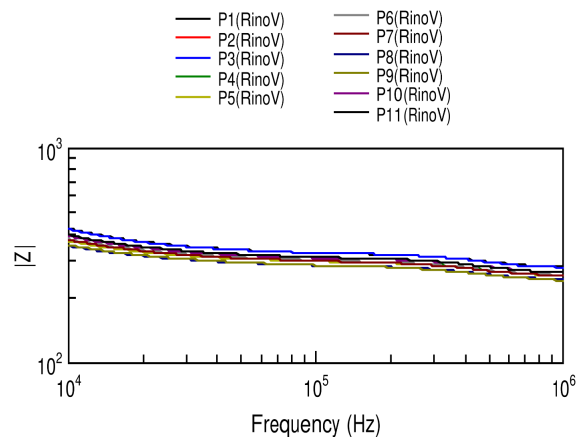


**Figure 7:** Bode diagrams corresponding to the 11 samples of viral rhinopharyngitis (Prepared in Zview).

### Results and discussion

Samples during infection with viral rhinopharyngitis (RinoV): The bioelectrical data obtained from the 11 nasopharyngeal samples with viral rhinopharyngitis had a sampling frame of 201 measurement points per biological sample submitted for analysis. In addition, a shunt resistance of 10 kΩ and an amplitude of 100 mV were used. As a result of these parameters, it was possible to obtain the Nyquist and Bode diagrams that we show below in Figure 6 and Figure 7.

It can be seen that in the graph shown in Figure 6 there is a slight observable difference in the Nyquist

diagram where each value of resistance ( $Z'$ ) and reactance ( $Z''$ ) are in some cases minimally different. Table 1 shows the respective values of impedance at the border frequencies, where the average value of the resistance for the frequency of 10 kHz is 349.89 Ω and for 1 MHz it is 256.39 Ω. In addition, the inflection points appear between the frequencies of 158 kHz to 182 kHz (Table 2) having a characteristic range for resistive values that go from 319.65 ohm to 279.77 ohm and for reactive values that go from 32.727 ohm to 26.705 ohm. which makes it possible to study its behavior as a randle circuit and to characterize the sample.

Values of bioelectrical impedance analysis in sample (Viral Rhinopharyngitis)								
Sample	Frequency 10kHz				Frequency 1MHz			
	Z'o(Ω)	Z''o(Ω)	Z o(Ω)	θ°o	Z'f(Ω)	Z''f(Ω)	Z f(Ω)	θ°f
P1	376.96	190.31	422.28	-26.787	278.13	21.997	279	-4.522
P2	359.28	164.91	395.32	-24.655	236.71	20.333	264.49	-4.409
P3	374.75	189.44	419.91	-26.817	277.18	21.487	278.01	-4.4327
P4	341.06	147.61	371.63	-23.403	255.04	18.48	255.71	-4.1444
P5	337.95	150.31	369.87	-23.978	253.58	19.23	254.31	-4.3367
P6	345.36	153.01	377.74	-23.895	255.98	18.316	256.63	-4.0927
P7	343.95	150.59	375.47	-23.645	254.41	18.407	255.08	-4.1382
P8	326.13	132.68	352.09	-22.138	242.24	19.54	243.03	-4.6117
P9	328.7	134.04	354.98	-22.185	240.55	20.469	241.42	-4.8637
P10	355.41	162.88	390.96	-24.621	262.77	20.723	263.59	-4.5092
P11	359.28	164.91	395.32	-24.655	263.71	20.333	264.49	-4.409

**Table 1:** Numerical data corresponding to the bioelectric components obtained (Figures 6 and 7) at the initial frequency 10 kHz and final frequency 1 MHz (border frequencies).

Bioelectrical data of the turning point (Viral Rhinopharyngitis)			
Sample	Frequency (kHz)	Z'(Ω)	Z''(Ω)
P1	181.197	318.47	32.523
P2	177.83	304.13	30.86
P3	169.82	319.65	32.727
P4	165.96	293.61	27.437
P5	165.96	291.95	28.255
P6	173.78	293.78	29.413
P7	162.18	292.94	29.051
P8	158.49	280.29	26.705
P9	158.49	279.77	28.532
P10	173.78	302.63	29.225
P11	169.82	304.58	30.84

**Table 2:** Impedance data corresponding to the inflection point of the Nyquist diagram (Figure 6) for viral rhinopharyngitis samples.

**Healthy Nasopharyngeal Sample (Healthy):**

Below are the bioelectrical data obtained from the 10 nasopharyngeal samples during the healthy stage of the patient, which had a sampling frame of 201 measurement points per biological sample subjected to analysis, with a Shunt resistance of 10 kΩ and amplitude of 100 mV. As a result of these data, it was possible to obtain the Nyquist and Bode diagrams shown in Figures 8 and 9.

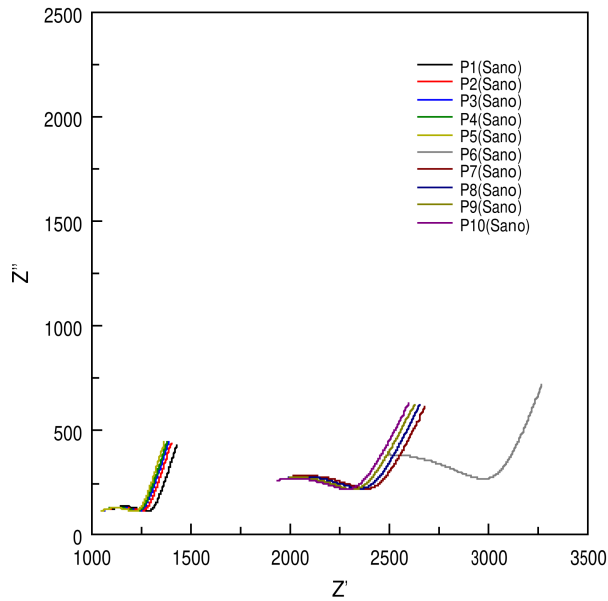


**Figure 8:** Nyquist diagrams corresponding to the 10 healthy nasopharyngeal samples (Prepared in Zview).

In the graph shown in Figure 8, a greater difference can be observed between the graphs of the samples in the Nyquist diagram, which could be due to the material extracted from the nasopharyngeal cavity since this does not present the previously analysed pathogenic agent. The most affected component in the graph is the resistive where we have ranges from 1427.8 4Ω to 2598 Ω for the initial frequency of 10 kHz and from 1100.5 Ω to 1933.7 Ω for the frequency of 1 MHz.

Finally, we can note that the values of the impedance module and phase angle corresponding to the Bode diagram of both samples with the pathogenic and healthy agent (Figures 7 and 9) remain equivalent with the correspondence of their resistance, in addition to presenting a clean behaviour and sinusoidal which would indicate that the samples are in a correct reading with a minimum of electromagnetic noise which causes errors or inconsistencies in the reading values by the biosensors.

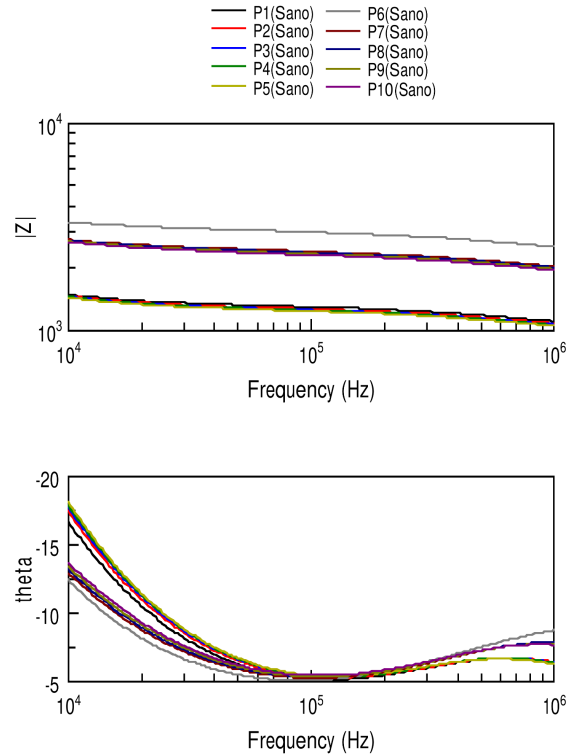


**Figure 9:** Bode plot obtained in healthy nasopharyngeal samples in a frequency range of 10 kHz to 1 MHz.

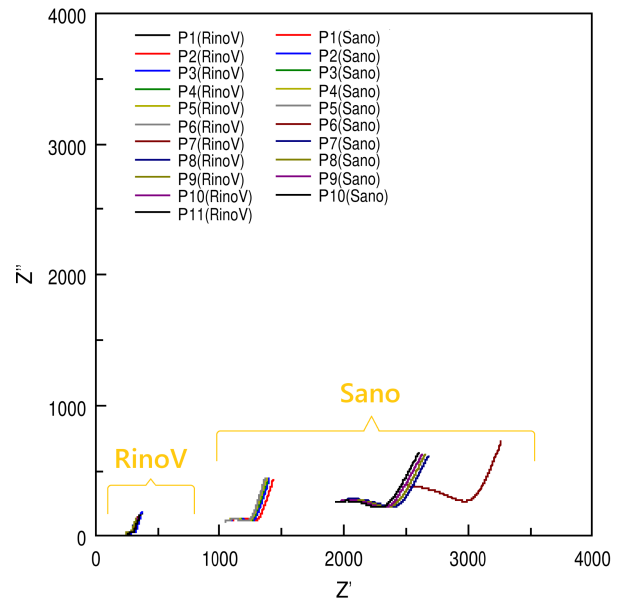


**Figure 10:** Nyquist diagram compared between all bioelectrical reading samples (Elaborated in Zview).

**Discussion**

From the aforementioned, the observable differences in the axis of the resistive impedance obtained from the values during the experimentation can be determined by means of a graph, which is shown in the Nyquist diagram (Figure 10).

In Figure 10, we noticed how viral samples tend to be closer to 0 Ω. However, it is known that existing bi-

ological agent shows a regulation to the flow of current, and this will have a resistive value that will never be absolute 0. For healthy samples, which do not present the rhinovirus, we can clearly notice that they tend to be greater than or equal to 1000 Ω. This is due to the fact that ordinary cells show a greater opposition to the flow of current through their internal components such as cell membranes, proteins, sugars among others [28].

Bioelectronic impedance analysis values in sample (Healthy)								
Sample	Frequency 10kHz				Frequency 1MHz			
	Z'o(Ω)	Z''o(Ω)	Z o(Ω)	θ'o	Z'f(Ω)	Z''f(Ω)	Z f(Ω)	θ'f
P1	1427.8	427.73	1490.5	-16.677	1100.5	124.84	1107.6	-6.4719
P2	1400.3	439.63	1467.7	-17.43	1076.1	122.69	1083.1	-6.5044
P3	1387.4	443.83	1456.7	-17.74	1061.6	119.94	1068.4	-6.446
P4	1380.6	446.31	1450.9	-17.915	1055.8	118.54	1062.4	-6.4061
P5	1367.3	448.62	1439	-18.165	1047.8	115.92	1054.2	-6.3131
P6	3266.3	721.78	3345.1	-12.461	2501.2	387.03	2531	-8.7961
P7	2679.8	617.41	2750	-12.974	2018	282.81	2037.7	-7.9777
P8	2650.5	623.07	2722.7	-13.229	1990.2	278.3	2009.6	-7.9603
P9	2626.8	627.08	2700.6	-13.427	1960.1	267.41	1978.3	-7.7687
P10	2598	633.4	2674.1	-13.702	1933.7	262.81	1951.5	-7.7397

**Table 3:** Bioelectrical data obtained in nasopharyngeal samples (healthy) for the extreme sweep frequencies shown in the previous graphs (Figures 8 and 9).

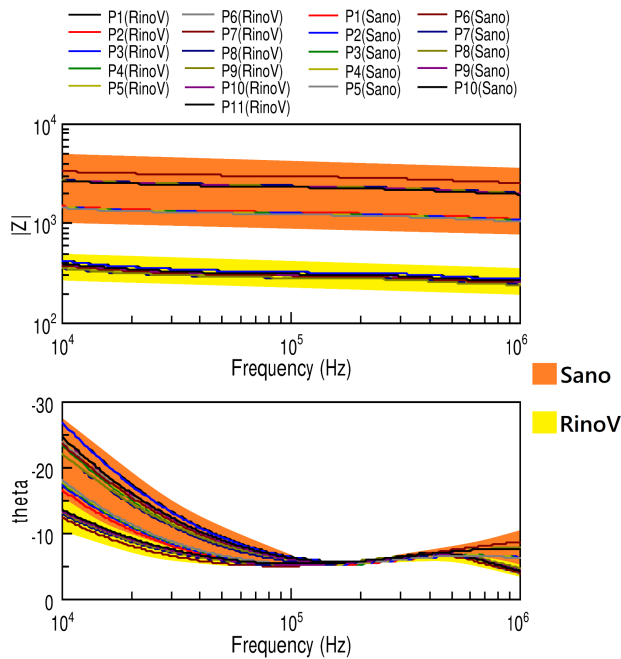


**Figure 11:** Bode diagram (Impedance Modulus and Phase Angle before frequency changes) comparing the bioelectrical response readings in Healthy and Contaminated samples (Prepared in Zview).

The data displayed on the bode plot (Figure 11) ensured that the bioimpedance readings were correct under little electrode noise. In addition, the difference in opposition to current flow is more clearly observed by comparing the impedance module, which has a start of reading greater than 10 kΩ when it is a healthy sample and less than 10 kΩ when the sample is infected. In the case of the Phase Angle, we can see its sinusoidal behaviour corresponding to a reading in biological material; however, it can be noted how the phase angle of the infected sample is less than the healthy sample at the frequency step to which it was subjected.

With the values obtained during the experimental stage, it was concluded that the behaviour of the rhinovirus is of a Randles circuit due to the inflection point that corresponds to the Warburg impedance (W). Which shows us a phenomenon of semi-infinite fusion that would be due to the moment where the flow of supplied electrons would cross the capsid of the virus when the frequency is in the range of 160 kHz and 190 kHz, giving us a characteristic response in the field as a result electrochemical. To characterize the circuit of the behaviour of the virus, the constant phase impedance element (ZCPE) must be considered due to its behaviour in the Bode diagram; once the important data was extracted, the Zview software was used to perform the appropriate bioelectri-

cal calculations that resemble the behaviour of the sample, resulting in the following bioelectrical scheme (Figure 12).

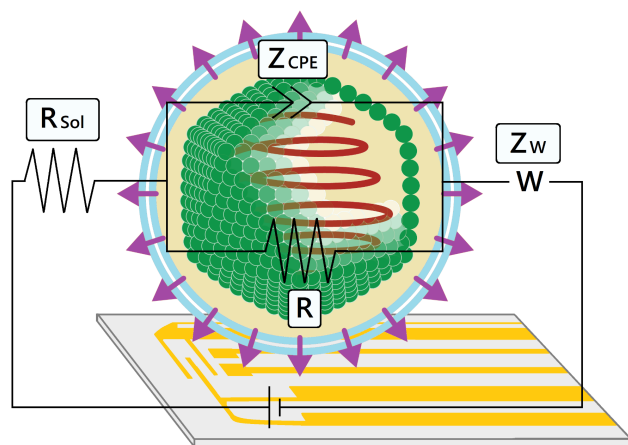


**Figure 12:** Electrical diagram of the nasopharyngeal sample considering the viral component as part of its usual reading (Created in GIMP and Zview).

Internal values of the Characterized Circuit		
Rsol		248,9
Z-CPE	CPE-T	$1,490 \times 10^{-10}$
	CPE-P	1,311
R		24,45
Z-W	Wo-R	81,17
	Wo-T	$5,9739 \times 10^{-6}$
	Wo-P	0,38994

**Table 4:** Values correspond to the components of the circuit modeled for the viral sample using the Zview software, with a Chi-Squared of 0.0043886 and Sum of Sqr of 1.7335.

The components of the characteristic bio circuit found have the following values shown in Table 4. Where CPE-T is the element of constant phase impedance with respect to time, CPE-P is the element of constant phase impedance with respect to frequency, R sol is the solution resistance, W-R the Warburg impedance with respect to Resistance, W-T the Warburg impedance with respect to Time and W-P the Warburg impedance with respect to Frequency.

## Conclusions

From the results, it can be extracted that the infected sample from the same patient has a behaviour of low resistance to the passage of electrons, this is due to the fact that the internal biology of the virus tends to facilitate the flow of current. Currently, these characteristics are used in transmission electron microscopes for metal marking, where viral agents are exposed to metallothionein, which finally ends up fusing with their proteins during incubation together with gold salts to finally obtain the production of electron-dense gold nanoclusters [27]. Due to this, it is confirmed that the impedance in the samples with the viral agent present a lower impedance value than the samples without the presence of the virus.

Finally, in this article, the basic bioelectric results of rhinovirus infection are presented. From the results obtained, it can be confirmed once again together with the results of other bioimpedance investigations, that the EIE or BIA method is a very viable alternative to be used in the future as a complete diagnostic method. From now on, more clinical studies are necessary to find factors to consider in order to improve this methodology, which has the potential to be a cutting-edge diagnostic methodology.

## References

- [1] J.R. Macdonald. *Impedance spectroscopy*. Ann Biomed Eng. 20(3):289-305. <https://doi.org/10.1007/bf02368532> (1992).
- [2] B.Y. Chang, S.M. Park. Electrochemical Impedance Spectroscopy. Annu Rev Anal Chem. 3(1):207-29. <https://doi.org/10.1146/annurev.anchem.012809.102211> (2010).
- [3] U.G. Kyle, I. Bosaeus, D.D. Lorenzo, P. Deurenberg, M. Elia, J.M. Gómez, et al. Bioelectrical impedance analysis—part I: review of principles and methods. Clin Nutr. 23(5):1226-43. <https://doi.org/10.1016/j.clnu.2004.06.004> (2004).
- [4] U.G. Kyle, I. Bosaeus, D.D. Lorenzo, P. Deurenberg, M. Elia, J.M. Gómez, et al. Bioelectrical impedance analysis—part II: utilization in clinical practice. Clin Nutr. 23(6):1430-53. <https://doi.org/10.1016/j.clnu.2004.09.012> (2004).
- [5] H.S. Jun, L.T.M. Dao, J.C. Pyun, S. Cho. Effect of cell senescence on the impedance measurement of adipose tissue-derived stem cells. Enzyme Microb Technol. 53(5):302-6. <https://doi.org/10.1016/j.enzmictec.2013.07.001> (2013).

- [6] U.T. Seyfert, H. Haubelt, A. Vogt, P. Hellstern. Variables influencing Multiplate™ whole blood impedance platelet aggregometry and turbidimetric platelet aggregation in healthy individuals. *Platelets*. 18(3):199-206. <https://doi.org/10.1080/09537100600944277> (2007).
- [7] M. Varshney, Y. Li. Interdigitated array microelectrodes based impedance biosensors for detection of bacterial cells. *Biosens Bioelectron*. 24(10):2951-60. <https://doi.org/10.1016/j.bios.2008.10.001> (2009).
- [8] J. Riera, P.J. Riu, P. Casan, J.R. Masclans. Tomografía de impedancia eléctrica en la lesión pulmonar aguda. *Med Intensiva*. 35(8):509-17. <https://doi.org/10.1016/j.medin.2011.05.005> (2011).
- [9] M. Ott, H. Fischer, H. Polat, E.B. Helm, M. Frenz, W.F. Caspary, et al. Bioelectrical Impedance Analysis as a Predictor of Survival in Patients with Human Immunodeficiency Virus Infection. *JAIDS J Acquir Immune Defic Syndr*. 9(1):20. <https://doi.org/10.1097/00042560-199505010-00003> (1995).
- [10] B.A. Boukamp. A package for impedance/admittance data analysis. *Solid State Ion*. 18-19:136-40. [https://doi.org/10.1016/0167-2738\(86\)90100-1](https://doi.org/10.1016/0167-2738(86)90100-1) (1986).
- [11] D.C. Jonscher. The Interpretation of Non-Ideal Dielectric Admittance and Impedance Diagrams. *Phys Status Solidi A*. <https://doi.org/10.1002/pssa.2210320241> (1975).
- [12] E.T. McAdams, J. Jossinet. Problems in equivalent circuit modeling of the electrical properties of biological tissues. *Bioelectrochem Bioenerg*. 40(2):147-52. [https://doi.org/10.1016/0302-4598\(96\)05069-6](https://doi.org/10.1016/0302-4598(96)05069-6) (1996).
- [13] R. Leake. Return difference bode diagram for optimal system design. *IEEE Trans Autom Control*. 10(3):342-4. <https://doi.org/10.1109/tac.1965.1098141> (1965).
- [14] C. Lexequías, B. Urcia, B. Franco, O. Baltuano, G. Patiño. Desarrollo de un espectrómetro de impedancia eléctrica portátil para análisis y caracterización del tejido sanguíneo. *Rev Investigación Física*. 24(1):9-16. <https://doi.org/10.15381/rif.v24i1.20241> (2021).
- [15] C. Lexequías, B. Urcia, L. Cisneros, S. Díaz, A. Peña, O. Baltuano, et al. Análisis de impedancia bioeléctrica en diferentes concentraciones de Glucosa Oxidasa (GOx). *Rev Investigación Física*. 24(2):54-62. <https://doi.org/10.15381/rif.v24i2.20427> (2021).
- [16] M.S. Le Gac, L. Delahaye, C. Martins-Carvalho, R. Marianowski. Rinofaringitis. *EMC - Pediatría*. 45(2):1-5. [https://doi.org/10.1016/s1245-1789\(10\)70176-1](https://doi.org/10.1016/s1245-1789(10)70176-1) (2010).
- [17] M.R. Rosas. Gripe y resfriado. *Clínica y tratamiento*. Offarm. 27(2):46-51. <https://www.elsevier.es/es-revista-offarm-4-pdf-13116051> (2008).
- [18] M. Álvarez Castelló, R. Castro Almarales, A. Abdo Rodríguez, S.D. Orta Hernández, M. Gómez Martínez, M.P. Álvarez Castelló. Infecciones respiratorias altas recurrentes: Algunas consideraciones. *Rev Cuba Med Gen Integral*. 24(1):0-0. [http://scielo.sld.cu/scielo.php?script=sci\\_arttext&pid=S0864-21252008000100011&lng=es&tlng=es](http://scielo.sld.cu/scielo.php?script=sci_arttext&pid=S0864-21252008000100011&lng=es&tlng=es) (2008).
- [19] Digilent WaveForms [Internet]. Disponible en: <https://store.digilentinc.com/digilent-waveforms/> (2023).
- [20] M.E. Moncada, M.P. Saldarriaga, A.F. Bravo, C.R. Pinedo. Medición de impedancia eléctrica en tejido biológico – revisión. *Tecnológicas*. 51-76. <https://doi.org/10.22430/22565337.113> (2010).
- [21] C. Lexequías, B. Urcia, A. Peña, O. Baltuano, G. Patiño. Application of Accu-Chek Test Strips as inexpensive microelectrodes for BIA research. *Rev Investigación Física*. 24(3):54-9. <https://doi.org/10.15381/rif.v24i3.20521> (2021).
- [22] P. Del Pozo, K. Abarca, I. Concha, J. Cerda. Concordancia del hisopado nasal con el hisopado nasofaríngeo en la detección de virus respiratorios por inmunofluorescencia directa. *Rev Chil Infectol*. 31(2):160-4. <https://dx.doi.org/10.4067/S0716-10182014000200006> (2014).
- [23] Guía de Atención Médica de Resfriado Común (Rinofaringitis Aguda). 1-9. [https://www.uis.edu.co/intranet/calidad/documentos/bienestar\\_estudiantil/guias/GBE.15.pdf](https://www.uis.edu.co/intranet/calidad/documentos/bienestar_estudiantil/guias/GBE.15.pdf) (2008).
- [24] Y. Sánchez. Guía clínica Rinofaringitis. E.S.E Hospital Nuestra Señora del Pilar, Medina. 1-10. <https://esehospitalmedina.gov.co/documentos/protocolos/consulta/guias/CE%20GU%2010%2020RINOFARINGITIS.pdf> (2014).

- [25] C. Greenham, K. Helms, W. Müller. Influence of Virus Infections on Impedance Parameters. *J Exp Bot.* 29(4):867-77. <https://doi.org/10.1093/jxb/29.4.867> (1978).
- [26] ZView® For Windows [Internet]. Scribner Associates. Disponible en: <https://www.scribner.com/software/> (2023).
- [27] K. Richert-Pöggeler, K. Franzke, K. Hipp, R. Kleespies. Electron Microscopy Methods for Virus Diagnosis and High Resolution Analysis of Viruses. *Frontiers in Microbiology.* <https://doi.org/10.3389/fmicb.2018.03255> (2019).
- [28] Marvels of Mucus and Phlegm [Internet]. NIH News in Health. Disponible en: <https://newsinhealth.nih.gov/2020/08/marvels-mucus-phlegm> (2020).